IET Microwaves, Antennas & Propagation

Research Article

IET Journals
The Institution of Engineering and Technology

Performance modelling and analysis for vehicle-to-anything connectivity in representative high-interference channels

ISSN 1751-8725
Received on 20th November 2018
Revised 26th July 2019
Accepted on 3rd September 2019
doi: 10.1049/iet-map.2018.6183
www.ietdl.org

Thomas Blazek[1] ✉, Golsa Ghiaasi[2], Christian Backfrieder[3], Gerald Ostermayer[3], Christoph F. Mecklenbräuker[1]

[1]*Institute of Telecommunications, TU Wien, Gusshausstraße 25, 1040 Vienna, Austria*
[2]*Department of Electronic Systems, NTNU Norwegian University of Science and Technology, IES, NO-7491 Trondheim, Norway*
[3]*Research Group Networks and Mobility, University of Applied Sciences Upper Austria, FH1, Softwarepark 11, 4232 Hagenberg, Austria*
✉ *E-mail: tblazek@nt.tuwien.ac.at*

Abstract: All too often, the performance of vehicular communications is benchmarked merely for a single link. A major challenge for benchmarking the performance of multiple interacting vehicles is the definition of repeatable vehicular scenarios. In this study, the authors propose and discuss an approach for performance analysis of the IEEE 802.11p standard in urban interference channels, by linking network simulations to a Software Defined Radio (SDR) setup. This approach provides communication performance measurements in the worst-case interference scenario caused by an urban traffic jam. They do this by starting out with vehicular traffic flow simulations and continue to model the medium access. They furthermore introduce an algorithm to reduce the complexity of the communication network while retaining its properties. Finally, they use a setup of SDR encompassing the communication nodes and channel emulators that emulate urban channels to measure the packet level performance as a function of signal-to-interference ratio and distance to a receiver under urban traffic conditions.

1 Introduction

Vehicular *ad-hoc* networks (VANETs) provide the potential to increase roadside safety by extending the ability to exchange information [1]. This can be used to convey warnings about roadside hazards, as well as communicate emergency manoeuvres that require quick reaction time. Especially in the second scenario, low latency requirements are in force which is difficult to meet using cellular communications. Hence, vehicular safety communications need to be able to communicate over an *ad-hoc* direct link. This link faces unique challenges. The outdoor physical channel sees large delay and Doppler spreads [2–4], providing challenging transmission conditions. On top of that, *ad-hoc* networks, due to the lack of a central scheduling authority, battle with interference. This interference is predominantly caused by nodes that do not know that they are transmitting in parallel to another node as they do not see each other. Hence, the problem is called the *hidden node* problem [5]. Thus, scalability is a major concern for VANETs [6]. As more and more cars will be equipped with vehicle-to-everything (V2X) technology, they still have to work in scenarios such as Fig. 1, where a traffic jam results in a very high node density.

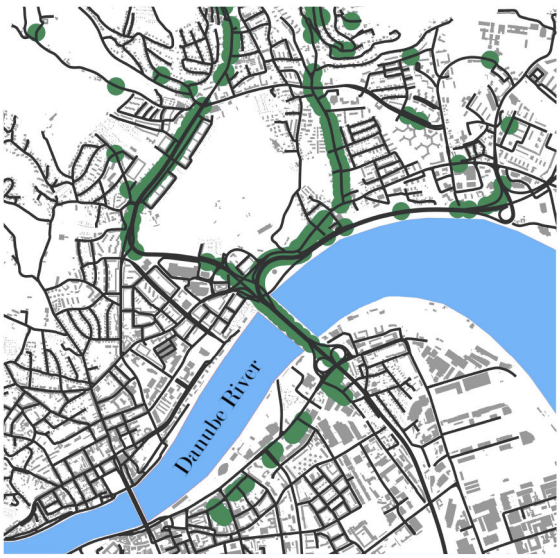

Fig. 1 *Traffic jam in Linz, Austria*

Due to the safety-applications tied to the system, comprehensive evaluations are required. Sometimes, this is done through measurement campaigns. However, testing large scale-vehicular networks in real life are both prohibitively expensive, and for many scenarios, not safe. Therefore, other means of testing are used. These include channel emulation to test nodes in labs, but this is usually done for small networks. On the other hand, large networks are often evaluated using network simulators, however they often do not portray the physics accurately.

Hence, a requirement exists for evaluating large scale networks, including physical channels, in a representative manner that allows accurate performance evaluations. For our analysis, we will focus on IEEE 802.11p [7], which is the first established *ad-hoc* standard for V2X communications.

1.1 Literature review

For evaluating single links and small networks, measurement campaigns are often conducted [8–11]. If this is not possible, emulation solutions are used instead [12–14]. These solutions, however, only evaluate small networks or single links. The complexity of such solutions becomes untenable for large networks. There, network-simulator based evaluations are conducted [15, 16].

IEEE 802.11p's default Medium Access Control (MAC) scheme, which is based on Carrier Sense Multiple Access with Collision Avoidance (CSMA/CA), combined with the need for frequent signalling of safety-relevant messages, has been contested on its scalability [6]. Furthermore, the ad-hoc nature leads to simultaneous channel access, resulting in interference at the receivers. The urban scenario is interesting in this case, as it is characterised by small distances between vehicles due to low speeds involved, as well as the strong geometric localisation of the vehicles. Hence, the scalability and the performance of IEEE

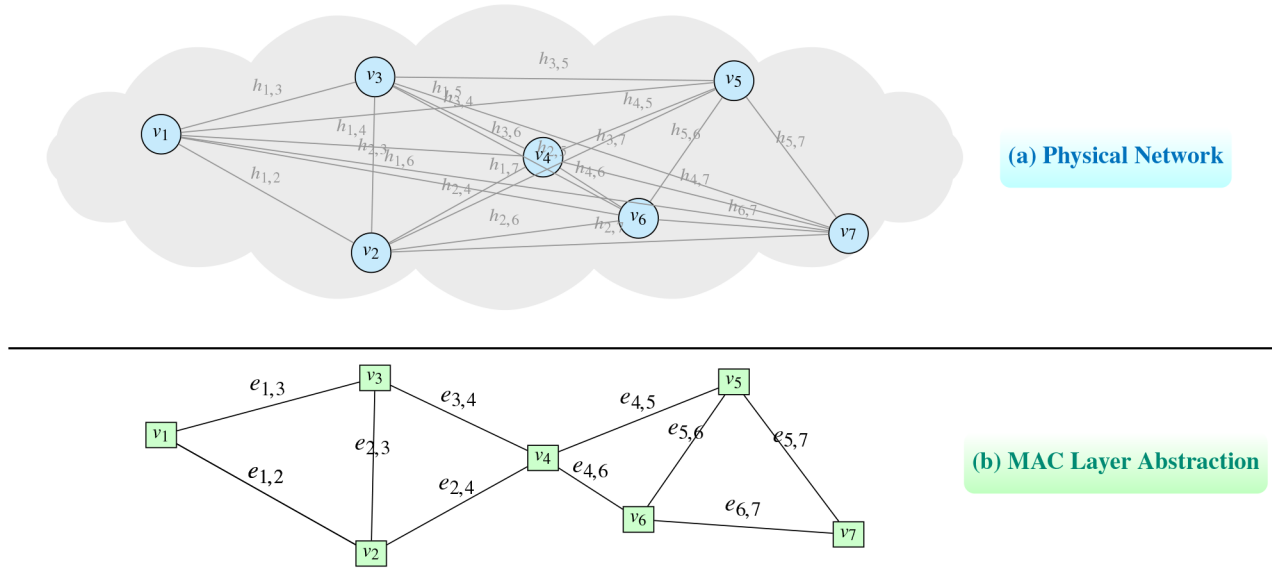

Fig. 2 *Representation of*
(a) Physical scenario with seven nodes, ***(b)*** As well as a MAC layer abstraction of the same scenario

802.11p have been a hot topic in research for the past years [17, 18].

Alternative channel access schemes were investigated [3] and the influence of hidden nodes was treated [19]. Most research, however takes a pure system-level approach, where the analysis is based on simulations and the influence of the physical channel is neglected. The vehicular physical channel itself has also been the centre of analysis [20, 21]. There, however, only a single link is considered, and the behaviour under the existence of interference is not demonstrated. Some advances in the analysis of interference in vehicular communications have been made, but they are either theoretic or simulation works [22, 23], or do not consider large scale networks, and focus on the interference between two nodes instead [24].

1.2 Our contribution

The main contribution of this paper is the combination of large-scale vehicular network simulations with a hardware setup to provide in-lab measured results on the influence of interference in urban scenarios. We achieve this by starting at large scale mobility simulations, and represent the resulting networks in a reduced complexity fashion that can be implemented on a small set of hardware nodes. [This is an extended version of our paper at EuCAP 2018 [25].]

We use OpenStreetMap [26] to obtain real-world street and building layouts of the city of Linz in Austria, and employ vehicular driving simulations [27] which provide us with real-life traffic scenarios. First, we use the MAC properties of IEEE 802.11p to describe and simulate the packet transmission and medium access under the assumption that all vehicles in the simulation are equipped with *ad-hoc* communication means, and simulate message propagation and collision in an *ad-hoc* network. Then, we approximate this behaviour through a graph representation in a way that allows us to represent transmission using a small number of devices. Finally, we use the simulated results to measure the performance of IEEE 802.11p on Software Defined Radios (SDRs) that act as transmitters, interferers, receivers and channel emulators. We use channel emulators with vehicular channel models, and analyse the packet error rate (PER), interferer number, signal-to-interference ratio (SIR) and distance to the receiver. This provides us with a realistic performance estimate of IEEE 802.11p in the challenging urban interference channels.

2 System model

Our aim is to model a large network of vehicles, for example the scenario shown in Fig. 1. In this scenario, the morning commuters want to cross the river from the north to the south, and only one highway bridge can be used. We assume these vehicles to be equipped with means for *ad-hoc* communications. Such a scenario, in general, has to be modelled like the physical layer representation in Fig. 2. Here, we have N nodes, and a total of $N(N-1)/2$ possible communication channels $h_{i,j}$. These channels are, due to the geometry and the mobility of the nodes doubly selective $h(t,\tau)$. We do however assume reciprocity, hence $h_{i,j} = h_{j,i}$.

For large networks, this model becomes unwieldy and computationally prohibitively expensive. Even when using only a 4-tap delay line as channel model, 40,000 multiplications and additions have to be computed for a single link for 1 packet of 500-byte length [28]. This number grows quadratically with the number of nodes in the network. Therefore, abstractions are introduced to keep the computational complexity low.

The first step to introducing these abstractions is to formulate communication as a general communication graph, as seen in the MAC layer abstraction Fig. 2. Here, we represent the vehicles as nodes v_i, and model general connections between the nodes as edges $e_{i,j}$. While these edges are linked to communication channels, they incorporate abstractions that will be detailed in the subsequent sections. By taking the set of all vehicles $V = \{v_1, v_2, \ldots, v_N\}$ and the set of all edges $E = \{e_{1,2}, e_{1,3}, \ldots, e_{N-1,N}\}$ we can construct the general communication graph [29]

$$G = (V, E)\,. \tag{1}$$

When modelling the physical network (Fig. 2*a*), V is the set of all vehicles $V = \{v_1, \ldots, v_N\}$. In this case, the graph is a complete graph, thus the edge set is given as $E = \{h_{i,j} \,|\, \forall i, j \in (1, \ldots, N) \times (1, \ldots, N)\}$. We call this the physical graph G_P. Based on this, we want to find graph abstractions for the considered communication system. The vertices and edges of this graph depend strongly on the underlying protocol. In this paper, we base our analysis on IEEE 802.11p, the vehicular extension of the 802.11 standard [7]. This standard employs Orthogonal Frequency-Division Multiplexing (OFDM) at 5.9 GHz at a bandwidth of 10 MHz.

2.1 Physical parameters and medium access control

We assume the physical layer (PHY) as defined by the 802.11p standard [7]. The standard defines a range of admissible transmit powers. In this paper, we choose 10 dBm effective isotropic radiated power (EIRP). This is a fairly typical choice [30]. 802.11p *senses* whether someone else is transmitting through the clear channel assessment (CCA). Here, the sensed received power is

compared to a threshold, and if the CCA remains below this threshold, the channel is deemed empty. Then, we can define that an edge is added to the edge set according to

$$e_{i,j} \in E' \equiv PL(v_i, v_j) < P_{\mathrm{Tx}} - \mathrm{CCA}\,. \tag{2}$$

Given this new edge set E' we can build the new communication graph G as an edge-induced subgraph of the physical graph

$$G = G_P[E']\,. \tag{3}$$

For our parameters, the edge is in the set if and only if the path loss from v_i to v_j is <90 dB. This edge does not imply that a transmitted packet would be received correctly. Instead, the edge is an important indicator for the MAC scheme.

For the MAC, IEEE 802.11p uses CSMA/CA. Therefore, a node only transmits when it perceives the channel to be empty. Whenever two vehicles are within this sensing range of each other, they will not transmit simultaneously. Hence, two nodes will not interfere exactly if they are connected by an edge.

Finally, if, for a given subset of nodes V_{sub}, the condition is fulfilled that there is an edge between all nodes, i.e.

$$v_i, v_j \in V_{\mathrm{sub}} \Rightarrow e_{i,j} \in E \quad \forall (i, j), \tag{4}$$

then we call V_{sub} a *clique* C. In a clique, no hidden nodes exist, and only one node will transmit at any given time, discounting timing offsets.

2.2 Representative channel performance model

On the MAC layer, the observed communication channel is defined by the observed packet error probability $P(\mathscr{E})$ [28]. This packet error probability depends mainly on the physical channel of the link, the used standard, as well as the presence of interference. However, different scenarios may lead to the same packet error performance and are thus indistinguishable at the MAC layer. For instance, the scenario in Fig. 2 is shown in Fig. 3*a*. The node v_2 transmits a packet to node v_4. Additionally, nodes v_5 and v_6 may choose to transmit and act as hidden nodes. Packet loss may occur due to the physical channel $h_{2,4}$ or the hidden node interference, which again depends on their communication channels. Therefore, the probability depends on three different channels, and sees packets incoming from three nodes. Finally, due to the MAC, the transmit timing of v_5 and v_6 depends also on v_7.

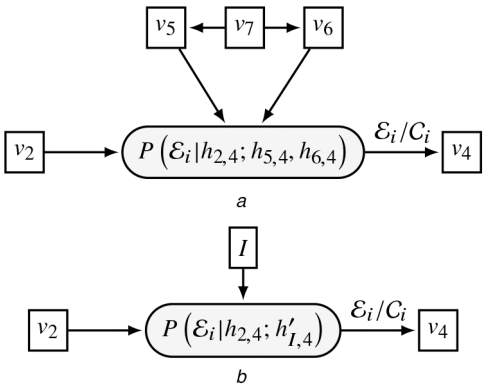

Fig. 3 *Two possible channel performance models representing the scenario in Fig. 2*
(a) Channel performance model of the original setup, ***(b)*** Alternative, representative setup

However, this channel can also be drawn as Fig. 3*b*. Here, only one interfering node I exists, with only one channel $h_{I,4}$. This node now represents the clique $I = \{v_5, v_6, v_7\}$. From this given clique, v_5 and v_6 are directly able to act as hidden nodes. Since only one of the nodes in the clique will transmit at any given time, a single node I can produce the traffic instead. It is important to note that in this example, the node v_7 is also important to capture. If this node transmits, the others will not, and thus, no hidden node transmission will occur from this clique. Crucially, if we model the transmission of v_7, but present it with a pathloss so large that the receiver does not sense the signal, we can model it as part of the interfering clique without changing the received statistics. Hence, all members of cliques have to be considered if even one node of a clique can act as hidden node. Then, the channel $h'_{I,4}$ has to adapt to the conditions of the currently transmitting node. We achieve this by setting a dynamic pathloss for every packet that ensures hidden transmissions from nodes that are too far away are below noise level. As long as models ***(a)*** and ***(b)*** lead to the same $P(\mathscr{E})$, they can be interchanged. Thus, ***(b)*** is *representative* of ***(a)***. Our goal in the following sections is to find a representative channel model for densely interfering channels that require as little nodes as possible.

3 Scenario data

In this section, we present the scenario considered in this paper, as well as our modelling approach. First, we introduce the traffic flow simulations on which our analysis is based. In a second step, we introduce the chosen assumptions about the communication channel. From this, we define a communication graph. Finally, we use the chosen PHY and MAC parameters to define a communication network, based on the relative vehicle positions obtained from the traffic simulations.

3.1 Traffic simulations

Before moving to network and channel modelling, we require data for geometric distributions of vehicles that provide us with a large number of interfering links. Thus, we have chosen a traffic jam scenario in an urban setting. The simulations to generate this scenario are conducted using the microscopic traffic simulator TraffSim [31]. The simulation setup presented in [27] consists of an excerpt of the city of Linz, with data gathered from OpenStreetMap. The simulation generates 3000 vehicles, whose start and endpoints are chosen at random in certain areas of the map, corresponding to commuter traffic from the northern side of the river to the southern side. Fig. 4 displays four snapshots at different simulation times. As there is a river between the two sides, and only one large bridge, a traffic jam occurs. This is especially critical at the northern end of the bridge, where two branches of a highway merge. As a longitudinal model, the intelligent driver model (IDM) is applied, and no coordination between the vehicles with respect to their routing is allowed.

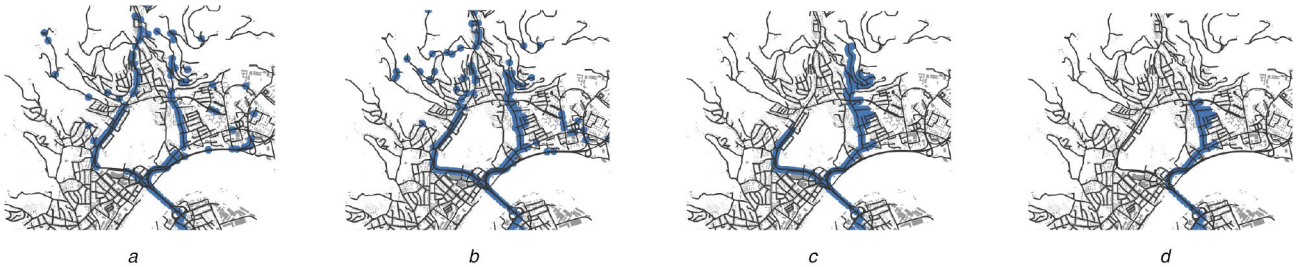

Fig. 4 *Four snapshots at different simulation times of the traffic flow simulation*
(a) 2000 s, ***(b)*** 5000 s, ***(c)*** 8000 s, ***(d)*** 11,000 s

3.2 Wireless channel modelling and emulation

Our goal in modelling the channel is to use models that are applicable to our scenario, yet remain general. We first address the pathloss model. For urban traffic, Karedal *et al.* proposed an empirical pathloss model for urban scenarios in [32] as

$$\begin{aligned} \mathrm{PL}_0 &= 20\log_{10}\frac{4\pi f_0}{c_0} \\ P(d) &= PL_0 + 16.8\log_{10}\left(\frac{d}{1\mathrm{m}}\right) + X_{\sigma_2} + \zeta \mathrm{PL}_c, \end{aligned} \tag{5}$$

where $f_0 = 5.9\,\mathrm{GHz}$, c_0 is the speed of light, X_{σ_2} is a lognormal model for shadowing, and ζ and PL_c account for stochastic shadowing. Using the map data, we can show that around the point of most interference, there are no large-scale obstructions, as it is surrounded by water on one side, and a large field on the other, and therefore we neglect the corresponding terms by setting X_{σ_2} and ζ to 0. The given pathloss coefficient in the model is smaller than 2, indicating that the authors observed waveguiding effects. With our chosen transmit power, CCA and this pathloss model, we arrive at a *sensing range* of 324 m, which is a plausible range [33]. Hence, we assume that the edge $e_{i,j}$ is part of the graph if the geometrical distance between v_i and v_j is below 324 m.

We account for small-scale fading using a tapped-delay line based channel emulator [34], therefore we use the delay line fading model which results in the time-variant impulse response

$$\mathscr{H}(t,\tau) = \sum_{i=1}^{N} \eta_i h_i(t)\delta(\tau - \tau_i), \tag{6}$$

where the parameters are set according to [35]. Specifically, we use a channel model defined for IEEE 802.11p, which uses four taps. While four taps are a low number of taps, it was shown to be a good trade-off between complexity and accuracy for a vehicular *ad-hoc* channel at narrow bandwidths [36]. The model furthermore uses asymmetric half-bathtub shaped Doppler spectra. These Doppler spectra account for the fact that different scatterer clusters are not positioned uniformly around the receiver, but tend to be seen only from one side. Since we do not assume shadowing, we use the *Urban LOS* model, for which the channel parameters are shown in Table 1. We do not account for small-scale fading variations in establishing communication graph, and thus the graph is based on median received powers.

3.3 Packet simulations

All vehicles are expected to communicate according to the parameters described in Section 2. The chosen MAC scheme distinguishes vehicles that *sense* a transmitter, i.e. vehicles whose received power is above a given threshold, even if the transmitted packet is not successfully decoded, from the others. For all vehicles that do sense each other, there will be no simultaneous transmissions. Thus, we generate the graph (1), width the edge placement according to (2), which translates to an effective communication range of 324 m.

On this graph, we simulate the Cooperative Awareness Message (CAM) beaconing according to the standard settings for safety-relevant messages [37], Access Class (AC) 3. Each node transmits 10 packets per second, which is given as maximum beaconing frequency in [38]. This is considered by ETSI as the baseline frequency that is defaulted to if the Distributed Congestion Control (DCC) algorithm is not actively shaping the cope of this work, hence we chose the default value. Thus, the results here show a pessimistic baseline with respect to channel load.

If two nodes that share an edge transmit simultaneously, they will choose a random back-off according to the standard and re-transmit. After seven failed transmission attempts, the message is discarded.

In our evaluations, we will consider both the cases, where only one communication channel can be used, as well as the case where the load can be distributed across three communication channels.

Table 1 Urban LOS delay line [35]

Tap	η_i^2, dB	τ_i, ns	$f_{i,d}$, Hz	Profile
$i = 1$	0	0	0	static
$i = 2$	−8	117	236	HalfBT
$i = 3$	−10	183	−157	HalfBT
$i = 4$	−15	333	492	HalfBT

4 Modelling a representative channel

Our goal now is to find a low complexity representative channel for the scenario described in the previous section. Considering an approach analogous to Fig. 3, we want to find a channel representation with as few nodes as possible, and a manageable complexity with regard to the involved communication channels. We approach this at two levels. First, we define an algorithm that approximates the communication graph by a graph of simpler structure. Then, we analyse our chosen channel model with respect to implementation properties.

4.1 MAC level approximation

On the MAC level, the difficulty is that the communication graph, in general, is *connected*, i.e. there is a path of edges from every node v_i to every node v_j. Thus, for every packet transmission, the full network has to be considered and modelled. On the other hand, as discussed, a clique C is flexible to model, because no matter how many nodes are in a clique C, only one will transmit at any given time. Therefore, a clique can always be modelled by 1 representative node.

To achieve a simplified graph structure, we now present an algorithm that iteratively constructs cliques, and removes unimportant edges, with the end result of having a strongly simplified structure while a remaining representative for the original channel. We use two parameters as a performance indicator for the algorithm:

i. The probability mass function (PMF) of simultaneously incoming packets.
ii. The median channel access delay.

The first performance indicator, on the one hand, informs us about how often hidden node interference happens, and how many hidden node packets arrive simultaneously across the whole simulation. Thus, we can evaluate whether the overall number of interferers has been maintained through the approximation process. The second performance indicator, on the other hand, tells us how busy the channel in the *sensing range* is. This is a measure for the number of communication neighbours has been maintained.

Our devised algorithm is presented in Algorithm 1 (see Fig. 5). As input, it takes the original communication graph G_O constructed according to our listed conditions.

The algorithm begins by finding all cliques of maximal size (a clique is of maximal size if no node $v_i \in V \setminus C$ can be added such that C remains a clique) [39]. These cliques will, in general overlap. For example, in the graph in Fig. 2, both $c_1 = \{v_1, v_2, v_3\}$ and $c_2 = \{v_4, v_2, v_3\}$ are overlapping maximal cliques. The result is a *set* of maximal cliques C.

Next, we calculate the Szymkiewicz–Simpson coefficient, also called overlap index [40]

$$OL(A,B) = \frac{|A \cap B|}{\min(|A|, |B|)}, \tag{7}$$

which measures how much of the smaller of two sets is also contained in the larger one. If two cliques are strongly overlapping, we can merge them into one superclique without changing much about the overall statistics. Conversely, if they are very loosely overlapping, we can separate them entirely to remove crosstalk, and still not change much about the transmission statistics.

1: **procedure** APPROXIMATED GRAPH(Graph G_O)
2: $C \leftarrow$ maxcliques(G_O)
3: **while** Overlap between cliques exists **do**
4: **for all** $\{(i,j) \,|\, \mathrm{OL}(c(i), c(j)) < t\}$ **do**
5: $o \leftarrow c(i) \cap c(j)$ ▷ Calculate overlap between $c(i)$, $c(j)$
6: $c(j) \leftarrow c(j) \setminus o$ ▷ Remove overlap from smaller clique
7: **end for**
8: **for all** $\{(i,j) \,|\, \mathrm{OL}(c(i), c(j)) \geq t\}$ **do**
9: $c(i) \leftarrow c(i) \cup c(j)$ ▷ Merge smaller into larger clique
10: $C \leftarrow C \setminus c(j)$ ▷ Remove smaller clique
11: **end for**
12: **end while**
13: **return** constructgraph(C)
14: **end procedure**

Fig. 5 *Algorithm 1: clique graph approximation*

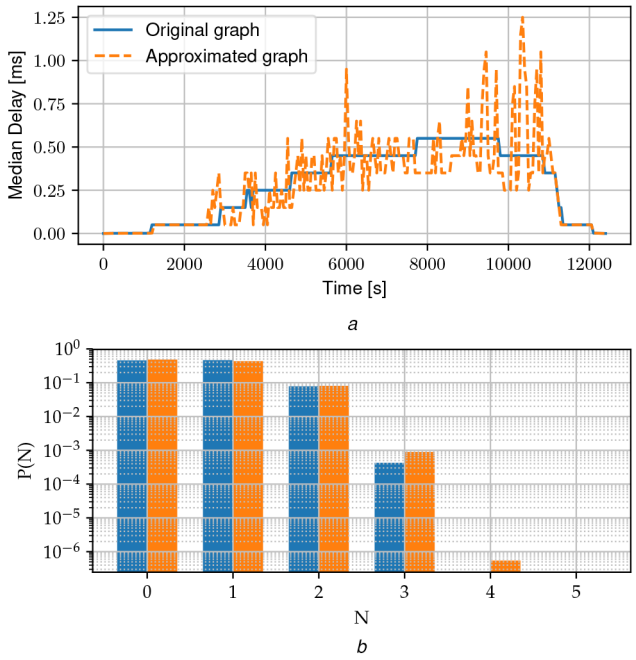

Fig. 6 *Graph approximation evaluation*
(a) Median channel access delay, ***(b)*** Probability of N incoming packets

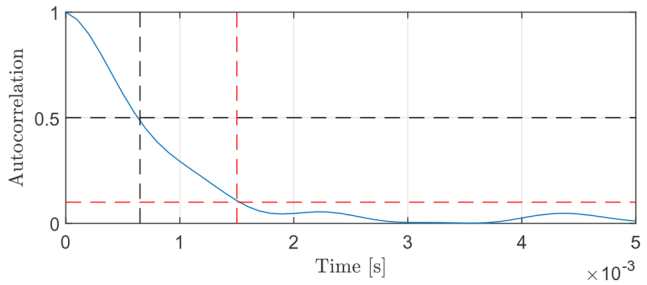

Fig. 7 *Autocorrelation function of the frequency domain channels*

Therefore, starting from the largest clique that has an overlap with at least one other clique, we evaluate this overlap index. If this index is below a given threshold t, we remove the overlap to make the cliques disjoint (Algorithm 1 (Fig. 5), lines 5 and 6). On the other hand, if the overlap is larger than t, we choose to merge the two cliques into one superclique (Algorithm 1 (Fig. 5), lines 9 and 10). This is done iteratively, until no overlap remains between any two cliques.

At the end, we construct a new, approximated graph from the cliques. In this approximated graph, the nodes are the same as in the original, but the edges are drawn if and only if two nodes are in the same clique.

In this state, the graph consists purely of cliques, which are disjointed since no overlap exists. Hence, no node of one clique can sense any node of any other clique. Since we eliminated any crosstalk, we can now represent each clique by 1 representative node.

To assess the performance of this algorithm, we now consider the performance metrics. We simulate the median channel access delay (Fig. 6*a*), as well as the probability of a node seeing N parallel incoming transmissions (Fig. 6*b*). The results show two noteworthy properties. The median statistics captures well the original apart from noise introduced due to this quantisation. Therefore, the approximated clique graph can be used as a graph with similar behaviour. Furthermore, both pose strongly similar collision probabilities. Finally, almost the full probability in both cases is concentrated in $N \in [0, 2]$, meaning that a node almost never sees more than two simultaneous incoming packets. Therefore, we argue that two transmitters can be used to effectively emulate the behaviour of a larger number of vehicles.

4.2 Channel approximation

As the system model in Fig. 2 shows, for N potentially incoming transmissions, we need to replicate N uncorrelated vehicular channels. With respect to small-scale fading, we assume all communications to follow the *urban approaching* channel model presented in Table 1. Thus, the N different channels $h_1(t,\tau), h_2(t,\tau), h_3(t,\tau), \ldots, h_N(t,\tau)$ are all realisations of one single channel model. We now assume $h'(t,\tau)$ to be a random realisation generated according to the modified sum-of-sinusoids approach given in [41] with a given seed. Then, due to the ergodic properties, we can instead take the N channels as $h'(t+\delta_1,\tau), h'(t+\delta_2,\tau), \ldots, h'(t+\delta_N,\tau)$. Here we use the same trace, with different random offsets δ_N. This approach works, as long as the δ_N are large enough for the channels to be decorrelated. Fig. 7 shows the autocorrelation function of the channel trace. Thus, we are below 50% correlation at 0.5 ms, and below 10% for 1.5 ms. Given that the packet transmissions we consider are 0.4–0.8 ms long, subsequent transmissions, even at the highest possible rate, see completely decorrelated channels within two to four transmissions. Hence, we argue, when analysing over suitably long durations, we can use a single small-scale fading channel emulator and transmit packets from a whole clique over the emulator. Due to the fast decorrelation of the channel, this will result in a performance that is equivalent to having a separate channel for each transmitting node individually.

5 Performance evaluation

In this work, we evaluate the performance for two scenarios. The first scenario is a simplified scenario in which a communication link sees a clique of hidden nodes. Thus, only one of the interferers is active at any given time, and the total interference load depends on the clique size. In this scenario, we consider constant interference power. This result provides us with baseline results about sensitivity to interference depending on the density of the surrounding network. In the second scenario, we consider a link in the presented traffic simulation, and evaluate the expected packet error rate as a function of simulation duration.

For our evaluation approach, we take advantage of results of the previous section, that shows that we can achieve representative channels with a small amount of nodes and channel emulators. This allows us to use physical nodes for transmitter, receiver and interferer, as well as physical hardware channel emulators. Thus, we can evaluate the presented scenarios through following measurements.

5.1 Measurement setup

As previously established, we only require a small number of nodes to evaluate the given scenarios. The lab setup we use is depicted in Fig. 8. The figure shows a photo and schematic of the employed measurement setup. As transmitter for our signal of interest, we use an Off-the-Shelf Modem (OTSM). For the

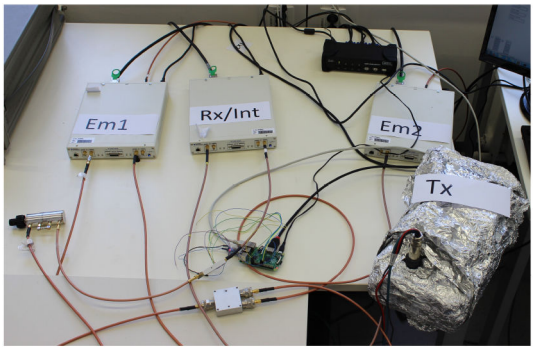

a

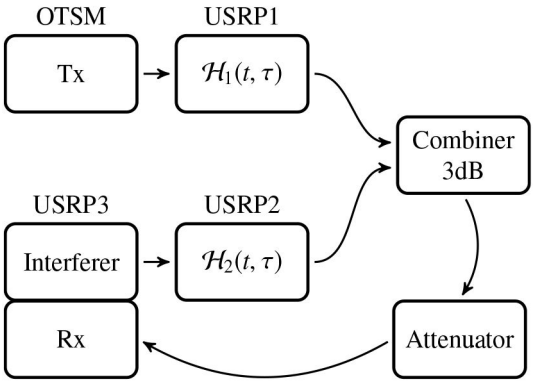

b

Fig. 8 *Measurement setup*
(a) Lab setup, ***(b)*** Schematic diagram of setup

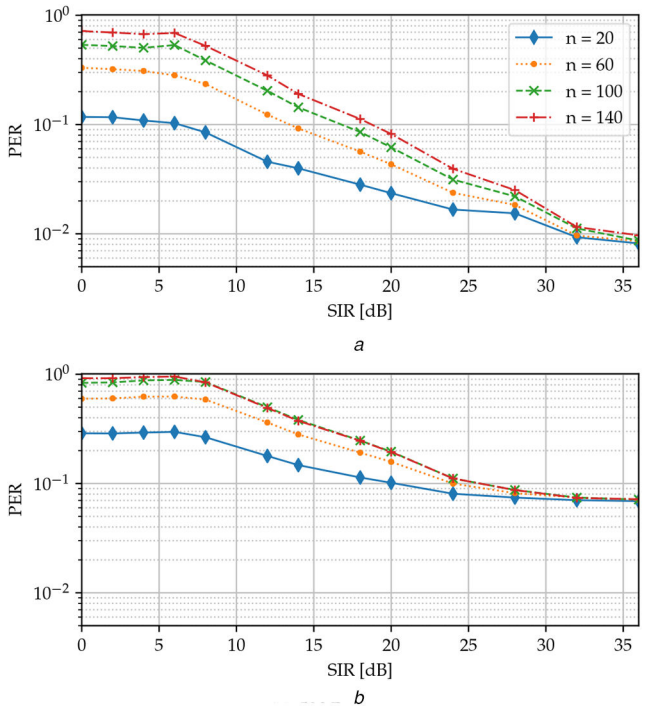

a

b

Fig. 9 *PER over SIR for interfering cliques of different sizes. For 500 bytes, no difference exists for 100 and 140 interferers*
(a) 258 Bytes, ***(b)*** 500 Bytes

interferer and receiver, we exploit the fact that National Instruments (NI) Universal Software Radio Peripheral (USRP)-2953R SDR have two separate radio-frequency daughter boards, which is why we can use one device for both functionalities. This USRP is running the 802.11 application framework, modified for 802.11p. We also use two further USRPs that run our custom channel emulator code. Both transmitter paths are combined through a power combiner, and passed through a final RADITEK RVATTN-DC-6 (0–70 dB) switched attenuator back to the receiver path of the USRP.

For a measurement run, the OTSM transmits a set number of 500,000 packets in a continuous stream. The interferer, on the other hand, has to transmit a pattern according to the full interfering clique. We achieve this by forwarding arbitrarily scheduled packets from a simulation trace via a Universal Datagram Protocol (UDP) socket to the transmitting node. This trace is generated by running the packet transmission simulations for a clique of the given size.

The two emulators are running the same small-scale fading trace, but with suitably decorrelated offsets. Since the interferer represents multiple nodes that may observe different pathloss values, the channel emulator in the interferer path additionally can switch path gain on a per millisecond basis to emulate this behaviour.

5.2 Performance under clique of hidden nodes

We first analyse the packet performance in the presence of a single clique with constant pathloss and size. We want to ignore the influence of additive noise, and therefore configure the transmitter to see Received Signal Strength Indicator (RSSI) at −50 dBm. This only leaves the influence of the small-scale fading, as well as the interference. We consider cliques of 40, 60, 100 and 140 vehicles that are using the same channel as the transmitting node. We evaluate the performance in terms of PER over the SIRs, which we define as the difference in decibels of the RSSIs, from 0 to 36 dB. We furthermore considered two different sizes for the packet transmissions (258 and 500 bytes). The packet sizes are chosen to reflect short and long packets that are possible within the specification for CAM messages. The smaller size of 258 bytes is given by the minimum packet size our hardware allows.

Fig. 9 shows the results of the measurements. All results show three distinct regions. Below $\simeq 6$ dB, the PER is constant. At these SIRs, the given PER is effectively a product of the error probability without interference and the probability of an interferer transmission overlapping with the transmission of interest. Due to the low SIR, any overlap is sufficient to lose the packet in the Cyclic Redundancy Check (CRC). At above 30 dB, we see a saturation of the performance for all clique sizes. This is where the interference becomes unnoticeable and the PER is caused completely by the small-scale fading channel. This saturation happens at very high SIRs because we are plotting over median values for both transmitter as well as interferer. Since we observe fading on both sides, even at high SIRs we frequently observe momentary dips that lead to packet loss. These two regions are connected by a linear transition.

5.3 Performance in traffic simulations

We now investigate the dynamic performance in the presented simulation traces. We do this by assuming a virtual roadside unit (RSU) at the interference hotspot, which is at the merging point of the two highways right before the bridge. The location of this virtual RSU is shown in Fig. 10. The figure also shows for a given time snapshot the clique assignments from the graph approximation. The blue clique is the clique of potential communication partners, while the orange and green clique are interfering cliques. Finally, the circle denotes the communication range.

To achieve the performance analysis, we analyse the achievable performance for different transmitter positions in 25, 50, and 100 m distance from the RSU. Fig. 11 shows the essential parameters for the interfering cliques calculated through our approximation algorithm. Fig. 11*a* shows the sizes of the three cliques of interest, while Fig. 11*b* shows the minimum and maximum distances from clique nodes to our virtual RSU. As all the considered roads are more or less straight, and the clusters are aligned along these roads, we can assume that the nodes are uniformly distributed between those minimum and maximum values. We use these distances for the interfering cliques to generate random pathlosses according to (5) along with random transmission events. For high pathloss (far distance), the interfering packet will not be seen by the receiver,

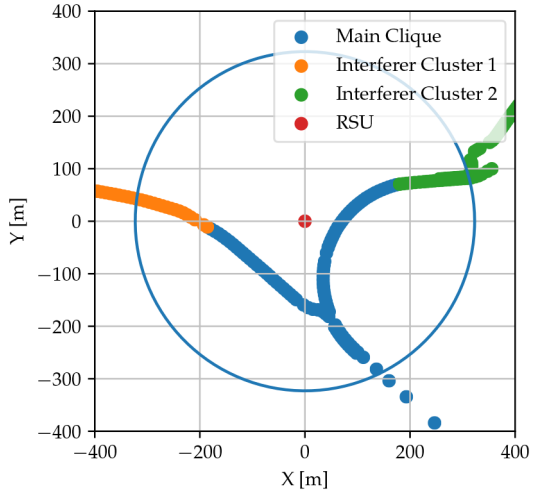

Fig. 10 *Snapshot of clique distribution*

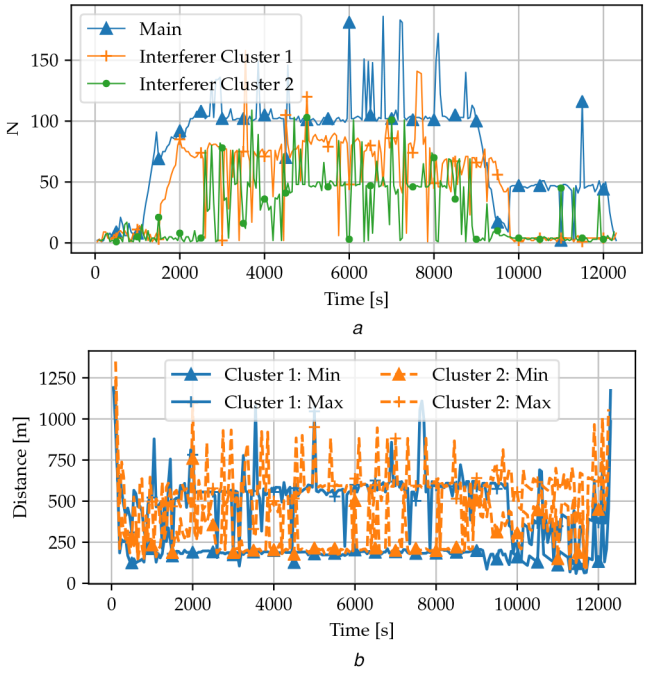

Fig. 11 *Change of clique parameters over the simulation time*
(a) Clique sizes, ***(b)*** Clique distances

while for low pathloss (close distance), the interfering packet will disturb communications. Due to the way we approximated the graph cliques, this approach will give us an interference pattern that is representative of the interference that will occur in the original network. The resulting parameters show that the simulation enters a relatively steady state at around 2500 s, and remains in this steady state for 6500 s. In this stationary regime, the first interfering clique sees $N \simeq 80$ nodes, and the second interfering clique sees $N \simeq 50$ nodes. Both cliques have distances distributed between 150 and 600 m from the RSU receiver. Hence, we concentrate on this stationarity region for our further measurements. To set the RSSI for the signal of interest, we evaluate (5) for distances of 25, 50 and 100 m. We use these distances, as well as the interferer distances, to draw a new random SIR value every 1 ms. This value is then achieved by setting the attenuation in the interfering channel emulator. This approach does not guarantee the interferer strength to change only between transmissions. We do however argue that, since we only apply this to the interfering nodes, the resulting PER is still representative for the scenario.

Using this approach, we now evaluate the scenario for both chosen packet sizes, and for the configurations with one usable channel and three usable channels [42]. The resulting PER as a function of time is shown in Fig. 12. The results show that within

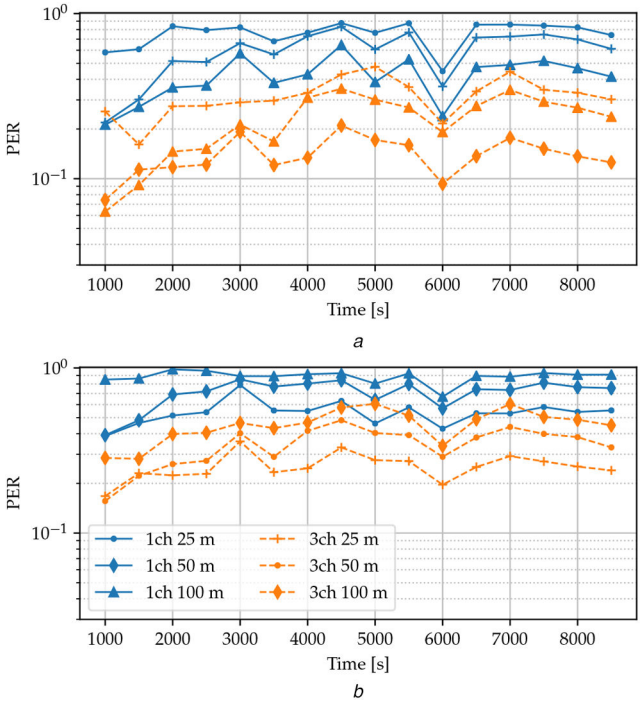

Fig. 12 *PER simulation time for one and three used channels, and distances of 25, 50 and 100 m to the receiver*
(a) 258 Bytes, ***(b)*** 500 Bytes

the stationarity region the resulting PERs assume an almost constant value, with small fluctuations caused by the fluctuations of the clique sizes. Furthermore, we do have a uniformly high packet loss, with only short packets, close to the receiver seeing a small amount of throughput. This can be easily understood, due to the large interfering clique sizes, and the relative proximity of the interferers. According to Fig. 9, an SIR well above 10 dB is required to see increasing performance. This is seldom achieved for the parameters of our simulation. The throughput can be improved by using short packets and three channels, however even then packet loss reaches >20% for a distance of 100 m to the receiver.

6 Conclusions

We presented an approach to simplify an *ad-hoc* communication system by introducing less complex, yet representative communication scenarios. Our results show that highly dense interference scenarios can be broken down using approximation algorithms, resulting in far less complex networks. These networks can then be used to conduct accurate performance analysis including PL and channel considerations. We exploit these results for measuring the behaviour of IEEE 802.11p under the influence of an urban interference channel. Our approach allows producing urban interference channel measurements in a lab setting using an equivalent scenario with a manageable amount of SDRs. We chose a scenario that is representative of the worst case that is encountered in urban communication scenarios, with severe traffic jams merging and no obstructions to reduce the interference. We confirm through measurements that without higher-layer control, IEEE 802.11p suffers severely in such a scenario. The use of multiple channels is required to allow communications, and algorithms like the DCC which control the transmit frequency, transmit power and receiver sensitivity are expected to ensure reception quality. Our results suggest that modifying these parameters is indeed required to achieve reliable packet delivery probabilities. The setup we presented here can be used to evaluate transmission parameters and test the resilience against interference in urban communication channels, and can contribute to finding a compromise between throughput and channel load.

7 Acknowledgments

The authors thank the CA15104 IRACON COST action for facilitating the exchange of knowledge.

8 References

[1] Alexander, P., Haley, D., Grant, A.: 'Cooperative intelligent transport systems: 5.9-GHz field trials', *Proc. IEEE*, 2011, **99**, (7), pp. 1213–1235

[2] Acosta-Marum, G., Ingram, M.A.: 'Six time-and frequency- selective empirical channel models for vehicular wireless LANs', *IEEE Veh. Technol. Mag.*, 2007, **2**, (4), pp. 4–11

[3] Ma, X., Chen, X., Hightower, P., *et al.*: 'The physical layer of the IEEE 802.11p WAVE communication standard: the specifications and challenges', *Electr. Veh., Model Simul.*, 2014, **II**, (3), pp. 1–8

[4] Meireles, R., Boban, M., Steenkiste, P., *et al.*: 'Experimental study on the impact of vehicular obstructions in VANETs'. Proc. IEEE Vehicular Networking Conf., Jersey City, NJ, USA, December 2010, pp. 338–345

[5] Sjöberg, K., Uhlemann, E., Ström, E.: 'How severe is the hidden terminal problem in VANETs when using CSMA and STDMA?'. 2011 Vehicular Technology Conf. (VTC Fall), San Francisco, CA, USA, September 2011, pp. 1–5

[6] Sjöberg, K., Uhlemann, E., Ström, E.: 'Scalability issues of the MAC methods STDMA and CSMA of IEEE 802.11p when used in VANETs'. In: Int. Conf. Communications Work, Capetown, South Africa, May 2010, pp. 1–5

[7] 'Information technology–Telecommunications and information exchange between systems Local and metropolitan area networks–Specific requirements Part 11: Wireless LAN Medium Access Control (MAC) and Physical Layer (PHY) Specifications', IEEE, 2012

[8] Sukuvaara, T.: 'Field measurements of IEEE 802.11p based vehicular networking entity'. Proc. 4th Int. Conf. Ubiquitous Future Networks, Phuket, Thailand, July 2012, pp. 135–139

[9] Bergenhem, C., Johansson, R., Coelingh, E.: 'Measurements on V2V communication quality in a vehicle platooning application', MACOM: International Workshop on Multiple Access Communications, Halmstad, Sweden, August 2017, pp. 35–48

[10] Shivaldova, V., Mecklenbräuker, C.F.: 'Real-world measurements-based evaluation of IEEE 802.11p system performance'. Proc. 5th IEEE Int. Symp. Wireless Vehicular Communications, Dresden, Germany, June 2013, pp. 1–5

[11] Schumacher, H., Tchouankem, H., Nuckelt, J., *et al.*: 'Vehicle-to-vehicle IEEE 802.11p performance measurements at urban intersections'. Proc. IEEE Int. Conf. Communications, Ottawa, ON, Canada, June 2012, pp. 7131–7135

[12] Fernandez-Carames, T.M., Gonzalez-Lopez, M., Castedo, L.: 'FPGA-based vehicular channel emulator for evaluation of IEEE 802.11p transceivers'. 2009 9th Int. Conf. Intelligent Transport Systems Telecommunications, Lille, France, October 2009, pp. 592–597

[13] Ghiaasi, G., Ashury, M., Xu, Z., *et al.*: 'Real-time vehicular channel emulator for future conformance tests of wireless ITS modems'. Proc. 10th European Conf. Antennas Propagation, Davos, Switzerland, April 2016, pp. 1–5

[14] Hofer, M., Xu, Z., Zemen, T.: 'Real-time channel emulation of a geometry-based stochastic channel model on a SDR platform'. Proc. of 18th Int. Workshop on Signal Processing Advances in Wireless Communications (SPAWC), Sapporo, Japan, July 2017, pp. 1–5

[15] Mittag, J., Papanastasiou, S., Hartenstein, H., *et al.*: 'Enabling accurate cross-layer PHY/MAC/NET simulation studies of vehicular communication networks', *Proc. IEEE*, 2011, **99**, (7), pp. 1311–1326

[16] Tripp-Barba, C., Urquiza-Aguiar, L., Estrada, J., *et al.*: 'Impact of packet error modeling in VANET simulations'. 2014 IEEE 6th Int. Conf. Adaptive Science Technology (ICAST), Ota, Nigeria, October 2014, pp. 1–7

[17] Stibor, L., Zang, Y., Reumerman, H.J.: 'Evaluation of communication distance of broadcast messages in a vehicular Ad-Hoc network using IEEE 802.11p'. Wireless Communications Networking Conf., Kowloon, China, March 2007, pp. 254–257

[18] Han, C., Dianati, M., Tafazolli, R., *et al.*: 'Analytical study of the IEEE 802.11p MAC sublayer in vehicular networks', *IEEE Trans. Intell. Transp. Syst.*, 2012, **13**, (2), pp. 873–886

[19] Zang, Y., Walke, B., Hiertz, G., *et al.*: 'IEEE 802.11p-based packet broadcast in radio channels with hidden stations and congestion control', arXiv preprint, arXiv:1612.03449, 2016, pp. 1–30

[20] Mecklenbräuker, C.F., Molisch, A.F., Karedal, J., *et al.*: 'Vehicular channel characterization and its implications for wireless system design and performance', *Proc. IEEE*, 2011, **99**, (7), pp. 1189–1212

[21] Bernado, L., Zemen, T., Tufvesson, F., *et al.*: 'Delay and Doppler spreads of nonstationary vehicular channels for safety-relevant scenarios', *Trans. Veh. Technol.*, 2014, **63**, (1), pp. 82–93

[22] Fazio, P., De Rango, F., Sottile, C., *et al.*: 'A new channel assignment scheme for interference-aware routing in vehicular networks'. 73rd Vehicular Technology Conf. (VTC Spring), Yokohama, Japan, May 2011, pp. 1–5

[23] Khan, I., Harri, J.: 'Can IEEE 802.11p and Wi-Fi coexist in the 5.9 GHz ITS band ?'. 18th Int. Symp. A World Wireless, Mobile Multimedia Networks, Macau, China, June 2017, pp. 1–6

[24] Fadda, M., Murroni, M., Popescu, V.: 'Interference issues for VANET communications in the TVWS in urban environments', *Trans. Veh. Technol.*, 2016, **65**, (7), pp. 4952–4958

[25] Blazek, T., Ghiaasi, G., Backfrieder, C., *et al.*: 'IEEE 802.11p performance for vehicle-to-anything connectivity in urban interference channels'. 12th European Conf. on Antennas and Propagation (EuCAP), London, UK, April 2018, pp. 1–5

[26] OpenStreetMap contributors: 'Planet dump retrieved from, 2017. Available at https://planet.osm.org

[27] Backfrieder, C., Ostermayer, G., Mecklenbräuker, C.F.: 'Increased traffic flow through node-based bottleneck prediction and V2X communication', *Trans. Intell. Transp. Syst.*, 2017, **18**, (2), pp. 349–363

[28] Blazek, T., Mecklenbräuker, C.F.: 'Measurement-based burst-error performance modeling for cooperative intelligent transport systems', *IEEE Trans. Intell. Transp. Syst.*, 2019, **20**, (1), pp. 162–171

[29] Blazek, T., Backfrieder, C., Mecklenbräuker, C., *et al.*: 'Improving communication reliability in intelligent transport systems through cooperative driving'. 10th IFIP Wireless and Mobile Networking Conf., Valencia, Spain, September 2017, pp. 1–6

[30] Paier, A., Faetani, D., Mecklenbräuker, C.F.: 'Performance evaluation of IEEE 802.11p physical layer infrastructure-to-vehicle real-world measurements'. Proc. 3rd Int. Symp. Applied Sciences Biomedical Communication Technologies, Rome, Italy, November 2010, pp. 1–5

[31] Backfrieder, C., Ostermayer, G., Mecklenbräuker, C.F.: 'Traffsim – a traffic simulator for investigations of congestion minimization through dynamic vehicle rerouting', *Int. J. Simul. Syst. Sci. Technol.*, 2014, **15**, (4), pp. 38–47

[32] Karedal, J., Czink, N., Paier, A., *et al.*: 'Path loss modeling for vehicle-to-vehicle communications', *Trans. Veh. Technol.*, 2011, **60**, (1), pp. 323–328

[33] Vivek, N., Srikanth, S.V., Saurabh, P., *et al.*: 'On field performance analysis of IEEE 802.11p and WAVE protocol stack for V2V & V2I communication'. Int. Conf. on Information Communication and Embedded Systems (ICICES2014), 2014, pp. 1–6

[34] Ghiaasi, G., Blazek, T., Ashury, M., *et al.*: 'Real-time emulation of nonstationary channels in safety-relevant vehicular scenarios', *Wirel. Commun. Mob. Comput.*, 2018, **2018**, pp. 1–11

[35] Blazek, T., Mecklenbräuker, C., Smely, D., *et al.*: 'Vehicular channel models: a system level performance analysis of tapped delay line models'. 15th Int. Conf. on ITS Telecommunications, Warsaw, Poland, May 2017, pp. 1–8

[36] Blazek, T., Zöchmann, E., Mecklenbräuker, C.: 'Millimeter wave vehicular channel emulation: a framework for balancing complexity and accuracy', *Sensors*, 2018, **2018**, pp. 1–21

[37] Eichler, S.: 'Performance evaluation of the IEEE 802.11p WAVE communication standard'. Vehicular Technology Conf., Baltimore, MD, USA, 30 September – 3 October 2007, pp. 2199–2203

[38] ETSI, T.: '102 637-2 v1. 2.1', Intelligent transport systems (ITS), 2011

[39] Lee, C., Reid, F., Mcdaid, A., *et al.*: 'Detecting highly overlapping community structure by greedy clique expansion', 2010

[40] Sharma, S., Singh, M.: 'Generalized similarity measure for categorical data clustering'. Int. Conf. Advances Computing Communications Informatics, Jaipur, India, September 2016, pp. 765–769

[41] Zemen, T., Mecklenbräuker, C.F.: 'Time-variant channel estimation using discrete prolate spheroidal sequences', *IEEE Trans. Signal Process.*, 2005, **53**, (9), pp. 3597–3607

[42] ETSI: 'EN 302 663 – V1.2.0 – intelligent transport systems (ITS); access layer specification for intelligent transport systems operating in the 5 GHz frequency band', ETSI, 2012